

# Measurement and prediction of mass transfer to experimental coral reef communities

M. E. Baird and M. J. Atkinson

Hawai'i Institute of Marine Biology, SOEST, University of Hawai'i, P.O. Box 1346, Kaneohe, Hawaii 96744

## Abstract

The uptake of nutrients (N and P) into coral reef communities is proposed to be limited by diffusion through concentration-depleted boundary layers between the water and organisms, or what is termed "mass transfer limitation." The mass transfer rate is a physical limit to the rate of nutrient uptake. Maximum uptake rates by highly rough biological surfaces have not yet been evaluated. Engineering correlations indicate that increased surface roughness should increase mass transfer, although it has been difficult to quantify roughness of living corals. In this paper, the effects of highly rough coral surfaces on mass transfer were investigated by using dissolution of gypsum (plaster-of-paris) from flat smooth surfaces and coral skeletons. The gypsum dissolution rates were measured as an increase in concentration of calcium ions in freshwater recirculating over experimental surfaces. Stanton numbers ( $St_m$ , a dimensionless number giving the ratio of uptake rate per unit area to the rate of advection of the substance past the uptake surface) of experimental smooth surfaces ranged from  $2.6$  to  $3.5 \times 10^{-5}$  and were the same as values in the engineering literature for smooth surfaces.  $St_m$  for coral-shaped surfaces ranged from  $70 \times 10^{-5}$  at  $0.03 \text{ m s}^{-1}$  to  $17 \times 10^{-5}$  at velocities up to  $0.50 \text{ m s}^{-1}$  and were in general  $9 \pm 1$  times that of smooth surfaces. The measured  $St_m$  for each coral-shaped surface was the same as the predicted  $St_m$  ( $\pm 10\%$ ) calculated from measured friction and roughness using a correlation of heat transfer.  $St_m$  for ammonia uptake on living coral reef communities show the same relationship between mass transfer, friction, and roughness as the coral-shaped gypsum surfaces. The transport rates of nutrients to reef surfaces are controlled by large-scale roughness, typically associated with coral heads, and not small-scale roughness elements on the organisms, nor biological alterations of diffusive boundary layers. Nutrient uptake and possibly other metabolic exchange rates are governed by concentration, water velocity, and friction dissipated over the reef, denoting that coral reef community metabolism is physically forced.

Uptake rates of nutrients ( $\text{PO}_4$ ,  $\text{NH}_4$ ) to assemblages of coral-reef benthos are positively correlated with the velocity of water flowing over the assemblage (Atkinson and Bilger 1992; Atkinson et al. 1994; Bilger and Atkinson 1995; Thomas and Atkinson 1997). These authors explained this observation by hypothesizing that the rate-limiting step for nutrient uptake is diffusion of nutrient ions through nutrient-depleted diffusive boundary layers adjacent to the surface of the benthos, termed mass-transfer limitation (Bilger and Atkinson 1992).

Nutrient-uptake rate of coral-reef benthos,  $m_s$  ( $\text{mol m}^{-2} \text{ s}^{-1}$ , where  $\text{m}^{-2}$  is the projected planar area of the bottom), is described as a first-order rate reaction with respect to the concentration gradient through the boundary layer:

$$m_s = S(C_b - C_w), \quad (1)$$

where  $C_w$  ( $\text{mol m}^{-3}$ ) is the concentration of the nutrient at the interface between the benthos and water,  $C_b$  ( $\text{mol m}^{-3}$ ) is the concentration of nutrient in the water beyond the diffusive boundary layer, and  $S$  ( $\text{m s}^{-1}$ ) is a boundary-layer mass-transfer coefficient.  $S$  can be partitioned into two parameters—the dimensionless Stanton number,  $St_m$ , and water velocity  $U_b$  ( $\text{m s}^{-1}$ )—thus introducing the dependence of nutrient uptake on water velocity,

$$m_s = St_m U_b (C_b - C_w), \quad (2)$$

## Acknowledgments

This research was in partial fulfillment of M. Baird's master's degree in the Department of Oceanography, University of Hawai'i at Manoa. Funding was from the Sea Grant Program, University of Hawai'i (ME/R year 2) to M.J.A. Thanks to Jim Fleming for his continued volunteer support of the flume research. This is HIMB contribution 1034 and SOEST contribution 4587.

where  $St_m$  is defined as the nutrient-uptake rate to the benthos ( $m_s$ ) divided by the advection of nutrient over the bottom [ $U_b(C_b - C_w)$ ] and is a measure of uptake performance of a projected area of benthos.

$St_m$  is usually determined under experimental conditions when  $C_w$  is negligible compared to  $C_b$ . In previous publications on nutrient uptake to coral reefs (Bilger and Atkinson 1995; Thomas and Atkinson 1997),  $St_m$  could only be estimated because  $C_w$  was not known. Nevertheless, conservative estimates of  $St_m$  for nutrient uptake (assuming  $C_w = 0$ ) were high compared to  $St_m$  from the engineering literature on mass transfer (Bilger and Atkinson 1992). Bilger and Atkinson suggested that high  $St_m$  may be due to biological mechanisms, such as active pumping of water through the boundary layer by microorganisms, or to geometric features of the benthos.

Recently, Thomas and Atkinson (1997) found that ammonia uptake to coral reef communities at high velocities could be predicted by assuming that  $C_w = 0$  and measuring friction and roughness and then calculating uptake using a heat-transfer relationship for sand-grain-roughened surfaces (Dipprey and Sabersky 1963). At lower velocities, however, Thomas and Atkinson (1997) found that the heat-transfer relationship underestimated ammonia uptake, and uncertainty remained as to whether this underestimation was due to geometric differences between Dipprey and Sabersky's experimental surface and a coral community or biological activity of the benthos.

The objective of the present research was to measure  $St_m$  accurately for coral-roughened surfaces. We chose to measure the dissolution of gypsum ( $\text{CaSO}_4 \cdot 2\text{H}_2\text{O}$ , commercially known as plaster-of-paris) from coral surfaces because (1) dissolution of gypsum is mass-transfer limited (Barton and

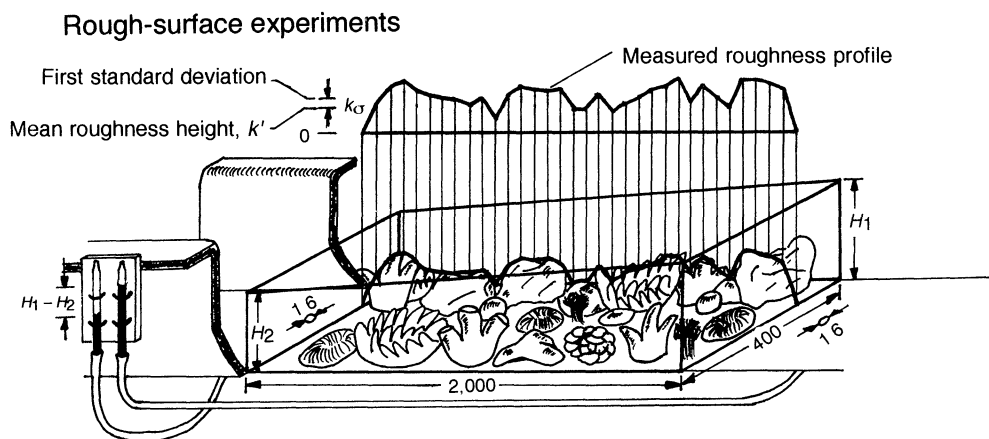


Fig. 1. Illustration of the flume (dimensions are in mm). Water was recirculated past gypsum-coated coral skeletons. The slope of the water surface, as measured by the difference in water height ( $H$ ), provided a measure of the friction dissipated by the benthic community. Mean and standard deviation of the height of the corals were measured by thin rods extended above the benthos.

Wilde 1971; Jokiel and Morrissey 1993; Thompson and Glenn 1994); (2) gypsum can be easily shaped; and (3) concentration of  $\text{Ca}^{2+}$  in the bulk water,  $C_b$ , and at the gypsum-coated coral surfaces or "wall,"  $C_w$ , could be determined. In this way, accurate measurements of  $\text{St}_m$  can be made for very rough surfaces, characteristic of coral-reef benthos, and compared to  $\text{St}_m$  for nutrient uptake to those surfaces.

The gypsum surfaces were placed in a flume and freshwater was recirculated.  $C_b$  was measured as  $\text{Ca}^{2+}$  concentration in the bulk flow, and  $C_w$  was calculated from saturated concentration of gypsum at the benthos-water interface. Changing  $C_b$  was used to determine  $m_s$  for the projected surface area. Thus,  $\text{St}_m$  could be calculated from Eq. 2.

## Methods

Experiments were conducted on smooth gypsum surfaces at velocities of  $0.2\text{--}0.84\text{ m s}^{-1}$  and on coral-rough gypsum surfaces at velocities of  $0.03\text{--}0.50\text{ m s}^{-1}$ . The smooth experiments were performed to validate the measurement of momentum and mass transport in the experimental flume with results from smooth surfaces reported in the engineering literature. The experiments on coral-rough surfaces were performed to accurately measure  $\text{St}_m$  of an inorganic surface that is geometrically similar to a coral community.

The experimental flume (Fig. 1) had a volume of  $2.3\text{ m}^3$  and channel dimensions  $24 \times 0.4 \times 0.2\text{ m}$ . Freshwater was recirculated using a variable-speed motor with a propeller. The projected planar surface area of the experimental surfaces varied from  $0.8$  to  $3.2\text{ m}^2$ , giving a volume to projected surface area ratio of  $0.72\text{--}2.9\text{ m}$ . The flume contained flow straighteners to dampen production of turbulence through the motor and turning sections.

**Smooth surfaces: Measurement of momentum transport—**For steadily flowing water in the experimental flume, the loss in gravitational potential energy of the water is equal to the energy dissipated as friction on all surfaces. The Manning formula (John and Haberman 1988) is an experimentally de-

rived relationship for the slope of the water surface as a function of velocity:

$$U_b = \frac{0.820}{n} \left( \frac{A_c}{P} \right)^{2/3} \sqrt{\sin \theta}, \quad (3)$$

where the term  $0.820/n$  has units of  $\text{m}^{1/3} \text{s}^{-1}$  (Manning roughness parameter,  $n$ , is  $0.01$  for a smooth surface; Chow 1959).  $\theta$  is the angle of the slope from the horizontal. For small  $\theta$ ,  $\sin \theta$  is approximately the slope of the water with the horizontal,  $s$  ( $\text{m m}^{-1}$ ).  $A_c$  ( $\text{m}^2$ ) is the cross-sectional area of the flow, and  $P$  ( $\text{m}$ ) is the perimeter of the flow experiencing a shear stress.

It is now convenient to define the commonly used Reynolds number,  $\text{Re}$ , a dimensionless parameter that is the ratio of inertia forces to viscous forces:

$$\text{Re} \equiv \frac{U_b D_h}{\nu}, \quad (4)$$

where  $U_b$  ( $\text{m s}^{-1}$ ) is the bulk velocity of the fluid over the surface,  $D_h$  ( $\text{m}$ ) is the hydraulic diameter, and  $\nu = 9 \times 10^{-7}$  ( $\text{m}^2 \text{s}^{-1}$ ) is the kinematic viscosity. The hydraulic diameter of the flume is (Kays and Crawford 1993)

$$D_h = \frac{4A_c}{P}. \quad (5)$$

For our empty flume with a smooth plaster-of-paris bottom,  $D_h = 0.4\text{ m}$ .

The slope,  $s$  ( $\text{m m}^{-1}$ ), of the water was determined from the mean of three measurements of the relative height of the water upstream and downstream of the test surface (Fig. 1). Two  $1.6\text{-mm}$  holes were drilled in the base of the flume,  $9\text{ m}$  apart. Tygon tubing ran from each hole to a central point, where the water height difference was measured on a Vernier scale to the nearest  $0.1\text{ mm}$  (Fig. 1). The tubing was flushed before reading to avoid gas buildup or thermal gradients, either of which could have changed the average density of the fluid within the tube. The bulk water velocity,  $U_b$ , of the flume was calculated from the mean of 10 measurements of

the time for a drogue to travel over 1 m of the experimental surface.

*Smooth surface mass transport: Determination of  $St_m$  smooth*—Experimentally there is a strong correlation between momentum transport and mass transport (Kays and Crawford 1993). The friction coefficient,  $c_f$ , a measure of momentum transport, is an important parameter in predicting mass transport.

For steadily recirculating water in the experimental flow, the loss of gravitational potential energy to friction can be written as

$$\rho g L W h s = \tau_w (L W + 2 L h) = \left( \frac{c_f}{2} \right) \rho U_b^2 (L W + 2 L h), \quad (6)$$

where  $\rho$  is density ( $\text{kg m}^{-3}$ );  $g$  is acceleration due to gravity ( $\text{m s}^{-2}$ );  $L$ ,  $W$ ,  $h$  are the length, width, and height (m) of the volume of water;  $s$  is the slope of the water ( $\text{m m}^{-1}$ ); and  $\tau_w$  is the wall shear stress ( $\text{N m}^{-1}$ ).  $c_f$  is the dimensionless friction coefficient, defined as

$$c_f \equiv \frac{\tau_w}{\rho U_b^2 / 2}, \quad (7)$$

where  $c_f$  is a dimensionless measure of the shear stress arising from both skin friction and form drag. The experimental flume is filled to  $h \equiv W/2$ , and solving for  $c_f$  from Eq. 6 and 7,

$$c_f = \frac{2 g W h s}{U_b^2 (W + 2 h)} \equiv \frac{g W s}{2 U_b^2}. \quad (8)$$

To compare measured  $St_m$  from different experiments and other studies, the Schmidt number,  $Sc$ , of the measured chemical species must be determined.  $Sc$  is the dimensionless ratio of the molecular diffusivity of momentum,  $\nu$  ( $\text{m}^2 \text{s}^{-1}$ ), to molecular diffusivity of mass,  $D$  ( $\text{m}^2 \text{s}^{-1}$ ), and is used in the correlation between momentum and mass transport:

$$Sc = \frac{\nu}{D}. \quad (9)$$

$Sc$  is a function of temperature,  $T$  (K), and ionic strength,  $I$ , and both must therefore be measured throughout the experiments. The relation between  $St_m$  and  $Sc$  for a smooth surface has been obtained by Stewart (1987), fitting the data of Shaw and Hanratty (1977) for  $1,730 < Sc < 37,200$ , and infinite dilution by

$$St_{m,smooth} = \sqrt{c_f} 2 (0.0575 Sc^{-2/3} + 0.1184 Sc^{-1}) \quad (10)$$

We use Eq. 3 to verify momentum transport to a smooth surface and Eq. 10 to verify mass transport to a smooth surface.

When gypsum ( $\text{CaSO}_4 \cdot 2\text{H}_2\text{O}$ ) dissolves from a surface,  $\text{Ca}^{2+}$  and  $\text{SO}_4^{2-}$  ions are released in equal quantities into solution, giving an approximately equal concentration in the recirculating water, or bulk solution:

$$[\text{Ca}^{2+}]_b = [\text{SO}_4^{2-}]_b. \quad (11)$$

The “wall” concentrations of these ions will be affected by the relative diffusivity of the two ions. The diffusivity of

$\text{Ca}^{2+}$  is lower than  $\text{SO}_4^{2-}$  (Li and Gregory 1974), and given the conditions of equal bulk concentration, equal flux, and a fixed diffusive sublayer thickness, the concentration gradient of  $\text{Ca}^{2+}$  is greater than  $\text{SO}_4^{2-}$ . The saturation state of gypsum at the surface must be shifted toward a higher concentration of  $\text{Ca}^{2+}$  relative to  $\text{SO}_4^{2-}$ .

The wall concentration of  $\text{Ca}^{2+}$  can be calculated by the following expansion and simplification of Eq. 2:

$$\begin{aligned} m_s &= St_{m,\text{Ca}} U_b ([\text{Ca}^{2+}]_w - [\text{Ca}^{2+}]_b) \\ &= St_{m,\text{SO}_4^{2-}} U_b ([\text{SO}_4^{2-}]_w - [\text{SO}_4^{2-}]_b). \end{aligned} \quad (12)$$

Water velocity,  $U_b$ , cancels from this equation. Dawson and Trass (1972) experimentally showed for a chemical species with high  $Sc$  that  $St_m = 0.0153 \text{Re}^{-0.12} \text{Sc}^{-0.68}$ .  $\text{Re}$  is equal for both  $\text{Ca}^{2+}$  and  $\text{SO}_4^{2-}$ , thus the ratio of  $St_m$  is

$$\begin{aligned} \frac{St_{m,\text{Ca}^{2+}}}{St_{m,\text{SO}_4^{2-}}} &= \frac{(\nu/D_{\text{Ca}^{2+}})^{-0.68}}{(\nu/D_{\text{SO}_4^{2-}})^{-0.68}} = \left( \frac{D_{\text{Ca}^{2+}}}{D_{\text{SO}_4^{2-}}} \right)^{0.68} \\ &= \left( \frac{7.93 \times 10^{-10}}{10.7 \times 10^{-10}} \right)^{0.68}_{\text{inf dilution}} = 0.816, \end{aligned} \quad (13)$$

where diffusivities of  $\text{Ca}^{2+}$  and  $\text{SO}_4^{2-}$  vary with ionic strength and temperature ( $\text{Ca}^{2+} = 7.82\text{--}7.96 \times 10^{-10} \text{m}^2 \text{s}^{-1}$ ;  $\text{SO}_4^{2-} = 10.45\text{--}10.85 \times 10^{-10} \text{m}^2 \text{s}^{-1}$ ; Li and Gregory 1974). The ratio of the concentration gradient is now simplified to a ratio of the diffusivities:

$$\left( \frac{D_{\text{Ca}^{2+}}}{D_{\text{SO}_4^{2-}}} \right)^{0.68} = \frac{([\text{SO}_4^{2-}]_w - [\text{SO}_4^{2-}]_b)}{([\text{Ca}^{2+}]_w - [\text{Ca}^{2+}]_b)}. \quad (14)$$

Substituting the equal bulk concentration condition (Eq. 11) and multiplying the whole equation by  $[\text{Ca}^{2+}]_w$  reveals a quadratic in which  $[\text{Ca}^{2+}]_b$  and  $[\text{SO}_4^{2-}]_w [\text{Ca}^{2+}]_w$  are measured and calculated, respectively:

$$\begin{aligned} \left( \frac{D_{\text{Ca}^{2+}}}{D_{\text{SO}_4^{2-}}} \right)^{0.68} [\text{Ca}^{2+}]_w^2 + \left[ 1 - \left( \frac{D_{\text{Ca}^{2+}}}{D_{\text{SO}_4^{2-}}} \right)^{0.68} \right] [\text{Ca}^{2+}]_b [\text{Ca}^{2+}]_w \\ - [\text{SO}_4^{2-}]_w [\text{Ca}^{2+}]_w = 0. \end{aligned} \quad (15)$$

The expression  $[\text{SO}_4^{2-}]_w [\text{Ca}^{2+}]_w$  is calculated from the concentration of  $\text{Ca}^{2+}$  and  $\text{SO}_4^{2-}$  ions at saturation in water. Concentrations of free ions or activities, which are calculated from total ion concentrations (Banz and Luthy 1985), are usually used to calculate solubility products,  $K_{sp}$ .  $\text{Ca}^{2+}$  diffuses from the surface as  $\text{Ca}^{2+}$  free ions and as  $\text{Ca}^{2+}\text{--}\text{SO}_4^{2-}$  ion pairs (Banz and Luthy 1985). Thus, it is appropriate to calculate the wall  $\text{Ca}^{2+}$  concentration from the total  $\text{Ca}^{2+}$  saturation concentration (Hardie 1967;  $\text{Ca}^{2+} \times \text{SO}_4^{2-} = 228\text{--}238 \text{mol}^2 \text{m}^{-6}$  during experiments). The positive root of Eq. 15 is the value for  $[\text{Ca}^{2+}]_w$ . By measuring  $U_b$  and  $[\text{Ca}^{2+}]_b$  over time,  $St_m$  can be calculated from Eq. 2. It is necessary to solve Eq. 15 at each interval throughout the experiment because diffusivity changes with temperature and ionic strength, and  $[\text{SO}_4^{2-}]_w [\text{Ca}^{2+}]_w$  changes with temperature.

The gypsum surfaces were prepared using US Gypsum No. 1 pottery plaster (% by weight: 96.2%  $\beta$ -hemihydrate  $[\text{CaSO}_4 \cdot \frac{1}{2}\text{H}_2\text{O}]$ , 0.5% calcium sulfate  $[\text{CaSO}_4]$ , 2.4% dolomite  $[\text{CaMg}(\text{CO}_3)_2]$ , 0.4% oxides, 0.5% acid insolubles),

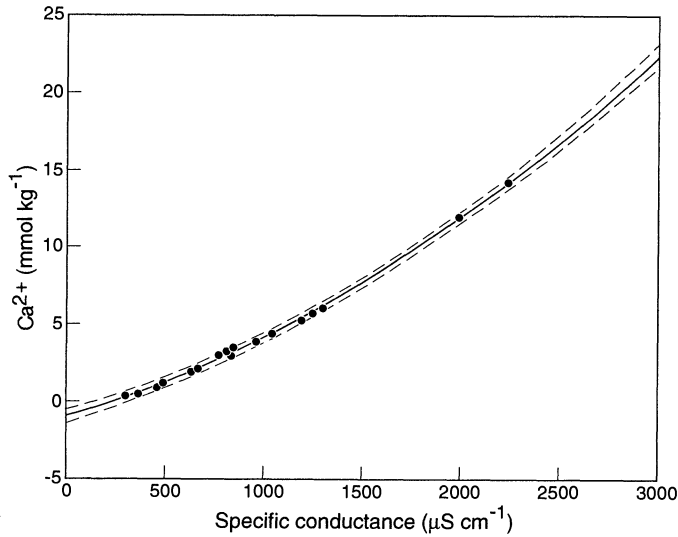
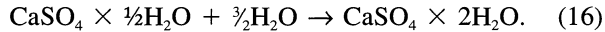


Fig. 2. Calcium concentration as determined by chemical titration vs. specific conductance ( $\mu\text{S cm}^{-1}$ ) calculated from CTD measurement of conductivity and temperature (K) over the 6 months of experiments. The 95% confidence limits are shown.

which is consistent with our own analysis by inductively coupled plasma/optical emission spectroscopy, ICP/OES (molar ratios: Ca:Mg:Na of 532:5.6:8).

The plaster powder was hydrated using tapwater in a 6:5 powder-to-water ratio by volume. The resulting reaction is



The plaster was then mixed vigorously for ~2.5 min and applied to the surface. Smooth surfaces were prepared by pouring the plaster directly into the flume and allowing it to set inside the flume overnight.

Water samples for  $\text{Ca}^{2+}$  determination were periodically taken throughout the experimental program, filtered using a GF/C glass-fiber filter, and then refrigerated until analyzed. Samples were analyzed for  $\text{Ca}^{2+}$ ,  $\text{Na}^{2+}$ , and  $\text{Mg}^{2+}$  concentrations using an ICP/OES, and for  $\text{Ca}^{2+}$  by potentiometric ion-selective electrode titrated with EGTA (Grasshoff et al. 1983). Both techniques measure total  $\text{Ca}^{2+}$  ions.

$\text{Ca}^{2+}$  was the only cation to change significantly in concentration throughout the experiments. Time, temperature, and conductivity were measured with a SeaBird Seacat 19 Profiler CTD. Specific conductance ( $\mu\text{S cm}^{-1}$ ), the conductivity measurement normalized to  $25^\circ\text{C}$ , showed a consistent fit to bulk  $\text{Ca}^{2+}$  (Fig. 2). Specific conductivity was therefore used as a measure of increasing  $\text{Ca}^{2+}$  in the recirculating water (Fig. 2). The points in Fig. 2 were taken from experiments over a 6-month period; there were no significant changes in the CTD calibration or the quality of the plaster.

**Rough surface experiments: Momentum transport**—When rough objects are placed in the bottom of the flume (Fig. 1), the friction due to the side walls becomes small compared with friction from the bottom. The flow acts as though the walls were not there because the presence of the smooth walls has only a small effect on flow compared to the rough bottom. This is a similar condition to an open channel, such

as a reef flat. An equation development as above for an open channel, describing the flume with a rough bottom, was given by Bilger and Atkinson (1992), with Eq. 5, 6, and 8 becoming

$$D_{h,\text{rough}} = 4h = 0.8m \quad (17)$$

$$\rho g L W h s = \tau_w L W = \left( \frac{c_f}{2} \right) \rho U_b^2 L W \quad (18)$$

$$c_f = \frac{2ghs}{U_b^2}. \quad (19)$$

Bilger and Atkinson (1992) chose Haaland's (1983) relationship, modified for an open channel, to describe the friction coefficient in terms of roughness height, height of the water, and Re:

$$(c_f/2)^{-1/2} = -5.1 \log_{10} \left[ \frac{6.9}{\text{Re}} + \left( \frac{k_s}{14.8h} \right)^{1.11} \right], \quad (20)$$

where  $k_s$  (m), the equivalent sand-grain roughness (Schlichting 1979), is defined as the solution of Eq. 20 from measured  $c_f$ , Re, and  $h$ .

The slope of the water surface was measured using the same manometer as for the smooth surface, but the coral sample was only 2–4 m long. For example, the measured water height difference for 2 m of coral skeletons included a height drop over 7 m of empty flume. An equivalent head for 9 m of coral was calculated as the measured head over 9 m less the head difference for 7 m of empty flume, times 9/2 (Eq. 21).

$$\Delta H_{\text{rough},9m} = \frac{9}{2} (\Delta H_{\text{measured},9m} - \Delta H_{\text{smooth},7m}). \quad (21)$$

**Rough surface experiments: Mass transport**—The two major nondimensional parameters that are used to describe surface geometry in engineering literature are wetted area to projected area ratio,  $\alpha$ , and the Reynolds roughness number,  $\text{Re}_k$ :

$$\alpha = \frac{\text{wetted surface area}}{\text{projected wall area}} \quad (22)$$

$$\text{Re}_k \equiv \frac{u^* k_s}{\nu} \quad (23)$$

where the friction, or shear velocity,  $u^*$ , is defined by

$$u^* = \sqrt{\tau_w / \rho} = U_b \sqrt{c_f / 2}, \quad (24)$$

where  $k_s$  is the effective sand-grain roughness, and a kinematic viscosity,  $\nu$ , of  $9 \times 10^{-7} \text{ m}^2 \text{ s}^{-1}$  has been used for calculations (Kays and Crawford 1993). It is usual that the calculated  $k_s$  is several times larger than a measured roughness scale (Dipprey and Sabersky 1963). While  $\alpha$  is perhaps the most appealing to use, Dawson and Trass (1972) have shown that for geometrically similar surfaces (i.e. equal  $\alpha$ ) in the same flow regime,  $\text{St}_m$  can differ. As a result,  $\text{Re}_k$  has been more successfully used and will be used with  $c_f$  as the roughness measure in this paper.

Dipprey and Sabersky (1963) developed correlations for

heat and momentum transfer in sand-roughened tubes. Bilger and Atkinson (1992) summarized this correlation as

$$St_{m,rough} = (c_f/2)/[0.9 + \sqrt{(c_f/2)/St_k}], \quad (25)$$

where  $St_k$ , the roughness Stanton number, is defined for  $70 \leq Re_k \leq 2,400$  as

$$St_k^{-1} = 5.19 Re_k^{0.2} Sc^{0.44} - 8.48. \quad (26)$$

Equation 25 gives  $St_{m,rough}$  as a function of  $Sc$  and geometric parameters  $Re_k$  and  $c_f$ .

Two sets of coral skeletons were used for coral-rough surface experiments. Coral skeletons were collected from the shore of Coconut Island, Kane'ohe Bay, Oahu, Hawai'i, and soaked in tapwater overnight before being coated with gypsum. The coral skeletons included *Porities compressa*, *Montipora capitata*, and *Fungia* sp. To make coral-rough gypsum surfaces, coral skeletons were dipped in plaster-of-paris as the water-plaster mixture hydrated. There was an approximately a 2-min period during plaster hydration in which quickly submerged coral skeletons could be completely covered with an even, 0.5–2-mm-thick coat of gypsum. The gypsum-coated corals were allowed to dry for 24 h before being placed in the flume for experimentation.

As well as determining an equivalent sand-grain roughness,  $k_s$ , for each experimental surface, an average roughness element height,  $k'$ , and the standard deviation of the roughness element height,  $k_\sigma$ , were measured.  $k'$  and  $k_\sigma$  were determined from measurement of the skeleton height above the flume bottom at 1-cm intervals along transects parallel to the flow (Fig. 1). Three 200-cm transects (600 points) were measured. The height of the water column from the bottom, minus the average roughness height,  $k'$ , was used to determine the average height of the water over the sample. Although  $k'$  and  $k_\sigma$  have been used before in Eq. 23 to determine  $Re_k$  (Thomas and Atkinson 1997), they resulted in a poor prediction of water slope using Eq. 20. Therefore predicted  $St_m$  was calculated using measurements of  $U_b$ ,  $c_f$ ,  $Re$ ,  $h$ , and  $Sc$  in Eq. 25, 26, 23, 24;  $k_s$  was determined from Eq. 20.

## Results

**Smooth surface: Momentum transport**—The head difference in the flume was predicted using the Manning formula (Fig. 3); thus, we confirmed accurate measurements of water slope and water velocity in the experimental flume.

**Smooth surface: Mass transport**—The flat gypsum surface placed in the bottom of the flume dissolved, releasing  $Ca^{2+}$  and  $SO_4^{2-}$  ions into the recirculating water. Thus,  $Ca^{2+}$  in the bulk water increase during the experiment and  $Ca^{2+}$  at the wall decreased (Fig. 4). Measured  $St_m$  and predicted  $St_m$  calculated from Eq. 10 decreased during the first 20 h as the interaction of temperature and ionic strength increased  $Sc$  (Fig. 4). The reported measured  $St_m$  (Table 1) for each surface and velocity was averaged over at least 20 min (10+ measurements). The largest errors in the measured  $St_m$  (5%) are from the measurements of water velocity and flume volume. The error in water velocity measurements is a consequence of the turbulent nature of the flow.

Values of  $St_m$  for flat, smooth gypsum surfaces in the

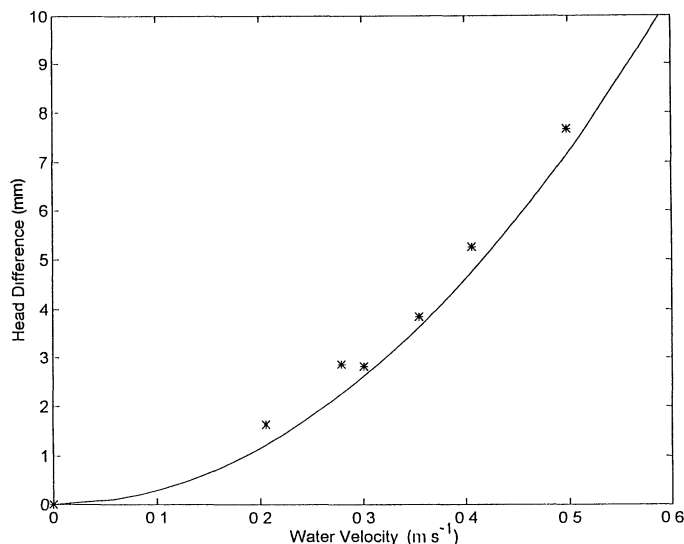


Fig. 3. Measured (\*) and predicted (—) head differences (Eq. 3) vs. water velocity for 9 m of the empty flume.

flume were  $2.9\text{--}3.5 \times 10^{-5}$  for velocities of  $0.20\text{--}0.84 \text{ m s}^{-1}$  and are within  $\pm 10\%$  of that calculated using Eq. 8–10. The consistency of our smooth  $St_m$  with values from engineering literature confirm our measurements of  $c_f$  and  $St_m$  in the experimental flume.

**Coral-rough surfaces: Momentum transport**—Coral skeletons were completely covered with gypsum throughout the measurement period (Fig. 5A). The two coral assemblages, gypsum corals A and B (Table 1), had mean roughness heights,  $k'$ , of 8.22 and 7.41 cm, respectively, and standard deviations of the mean height,  $k_\sigma$ , of 4.80 and 4.05 cm. The effective sand-grain roughnesses,  $k_s$ , calculated using Eq. 20 for each velocity in gypsum corals A No. 1 are 0.31, 0.29, 0.26, 0.30, 0.31, and 0.33 (Table 1), giving an average  $k_s$  of 0.30 m. Because the gypsum corals A Nos. 2–8 were conducted at a slightly lower average water velocity,  $c_f$  was estimated for each velocity using the relationship between  $U_b$  and  $c_f$  from No. 1, and an average  $k_s$  recalculated for Nos. 2–8 of 0.27 m. The measured head compares better with a predicted head using  $k_s$  of 0.27 m than using the measured roughness height,  $k'$ , of 8.22 cm (Fig. 6), as expected.

**Coral-rough surfaces: Mass transport**— $St_m$  for coral-rough gypsum surfaces ranged from  $22\text{ to }31 \times 10^{-5}$  at velocities  $>0.1 \text{ m s}^{-1}$ ,  $9 \pm 1$  times smooth gypsum surfaces (Table 1, Fig. 7). Much higher  $St_m$ , up to  $70 \times 10^{-5}$ , were measured for low water velocities (Table 1).  $St_m$  for the gypsum corals B at velocities of 0.26 and  $0.35 \text{ m s}^{-1}$  were  $17$  and  $19 \times 10^{-5}$ ,  $6 \pm 0.3$  times smooth surfaces.

The  $St_m$  measured for each coral community in group A corals was within the error of the predicted  $St_m$  ( $\pm 10\%$ ) from measured  $c_f$ ,  $Re_k$  (using  $k_s$ ), and  $Sc$  (Eq. 25).  $St_m$  measured was also positively correlated to  $St_m$  predicted (Fig. 8;  $P \ll 0.01$ ,  $r = 0.99$ ,  $n = 19$ ).

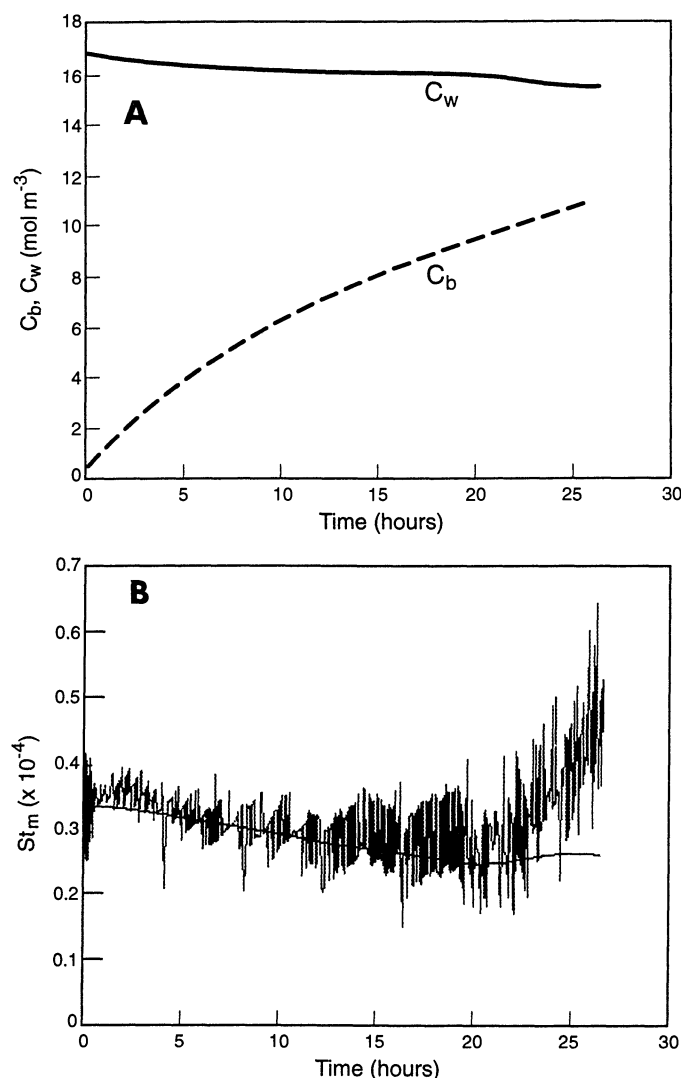


Fig. 4. (A) Concentration of total  $\text{Ca}^{2+}$  in the bulk,  $C_b$  (---), and, at the surface of the gypsum-coated corals,  $C_w$  (—) ( $\text{mol m}^{-3}$ ) vs. time (h) for flat gypsum No. 2. After 15 h the  $\text{Ca}^{2+}$  concentration gradient between the saturated wall and the near-saturated water approaches zero, resulting in the  $St_m$  (Eq. 2) heading toward infinity. The reported results from all experiments are within the first 5 h of the experiments. (B)  $St_m$  for a smooth surface (flat gypsum No. 2, Table 1) vs. time (h). The prediction by Stewart (1987) Eq. 10 (---) has been extrapolated to lower  $Sc$ .  $Sc$  for  $\text{Ca}^{2+}$  varied from 1,300 to 2,100 as a result of  $\nu$  varying from  $9$  to  $10.5 \times 10^{-7} \text{ m}^2 \text{ s}^{-1}$  and  $D_{\text{Ca}}$  from  $7.8$  to  $8.0 \text{ m}^2 \text{ s}^{-1}$  with changes in temperature and ionic strength.

## Discussion

The Manning equation (Eq. 3) predicts head difference and hence  $c_f$  for smooth surfaces (Fig. 3). As stated earlier, Eq. 20 did not predict head difference on coral-rough surfaces using the measured  $k'$  or  $k_s$  as roughness heights. Instead, the effective sand-grain roughness,  $k_s$ , was used (Fig. 6). Calculated values of  $k_s$  for the group A corals are greater than the depth of the water in the flume but substantially less than the hydraulic diameter,  $D_h$  ( $\sim 0.5 \text{ m}$ ), which is the

Table 1. Summary of experimental results for gypsum-dissolution experiments. There are three experimental surfaces: smooth-flat gypsum, coral-skeletons group A, and coral-skeletons group B. The experimental numbers indicate different coatings of gypsum on the same skeletons. Gypsum skeletons sanded with coarse sandpaper to create randomly oriented 1-mm grooves on coral-rough surface are indicated by an asterisk.

| Experimental surface | $U_b$<br>(m s <sup>-1</sup> ) | $C_f$<br>(×10 <sup>-3</sup> ) | Sc          | $St_m$<br>(×10 <sup>-5</sup> ) |
|----------------------|-------------------------------|-------------------------------|-------------|--------------------------------|
| Flat gypsum          |                               |                               |             |                                |
| No. 1                | 0.21                          | 8.4                           | No data     |                                |
|                      | 0.28                          | 8.0                           |             |                                |
|                      | 0.30                          | 6.8                           |             |                                |
|                      | 0.36                          | 6.7                           |             |                                |
|                      | 0.41                          | 7.0                           |             |                                |
|                      | 0.50                          | 6.8                           |             |                                |
| No. 2                | 0.29                          | 7.3                           | 1,300–2,100 | 3.5–3.0                        |
| No. 3                | 0.20                          | 8.0                           | 1,360       | 2.9                            |
|                      | 0.24                          | 7.6                           | 1,360       | 2.9                            |
|                      | 0.26                          | 7.5                           | 1,370       | 2.9                            |
|                      | 0.29                          | 7.3                           | 1,370       | 2.9                            |
|                      | 0.37                          | 7.1                           | 1,380       | 2.9                            |
| No. 4                | 0.35                          | No. 1 data used               | 1,360       | 2.9                            |
|                      | 0.84                          |                               | 1,410       | 3.0                            |
|                      | 0.69                          |                               | 1,440       | 2.6                            |
| Gypsum corals A      |                               |                               |             |                                |
| No. 1                | 0.15                          | 107                           | No data     |                                |
|                      | 0.29                          | 100                           |             |                                |
|                      | 0.36                          | 88.6                          |             |                                |
|                      | 0.38                          | 105                           |             |                                |
|                      | 0.44                          | 109                           |             |                                |
|                      | 0.48                          | 118                           |             |                                |
| No. 2                | 0.14                          | No. 1 data used               | 1,250       | 26                             |
|                      | 0.38                          |                               |             |                                |
| No. 3                | 0.50                          |                               | 1,270       | 24                             |
|                      | 0.47                          |                               | 1,270       | 24                             |
|                      | 0.51                          |                               | 1,270       | 24                             |
|                      | 0.40                          |                               | 1,270       | 25                             |
|                      | 0.31                          |                               | 1,270       | 26                             |
| No. 4                | 0.32                          |                               | 1,290       | 25                             |
|                      | 0.24                          |                               | 1,340       | 25                             |
| No. 5                | 0.13                          |                               | 1,260       | 31                             |
|                      | 0.18                          |                               | 1,270       | 28                             |
|                      | 0.15                          |                               | 1,280       | 29                             |
| No. 6                | 0.19                          |                               | 1,320       | 25                             |
|                      | 0.26                          |                               | 1,340       | 22                             |
| No. 7                | 0.03                          |                               | 1,260       | 70                             |
| No. 8*               | 0.48                          |                               | 1,260       | 23                             |
| Gypsum corals B      |                               |                               |             |                                |
| No. 1                | 0.045                         | 233                           | 1,230       | 52                             |
| No. 2*               | 0.043                         | 207                           | 1,240       | 55                             |

relevant length scale. This approach is consistent with the development of correlations by Dipprey and Sabersky (1963). It is best to think of  $k_s$  as an algebraic term to predict  $c_f$  at high  $Re$  (Eq. 20). It is evident that trying to find a meaningful roughness scale for irregularly rough surfaces is very difficult. Roughness is best measured by  $c_f$  and  $Re$ .

To determine whether tiny roughness elements on corals influence mass transfer, two experiments at  $0.043$  and  $0.48 \text{ m s}^{-1}$  (Table 1) were conducted on a sand-paper-roughened

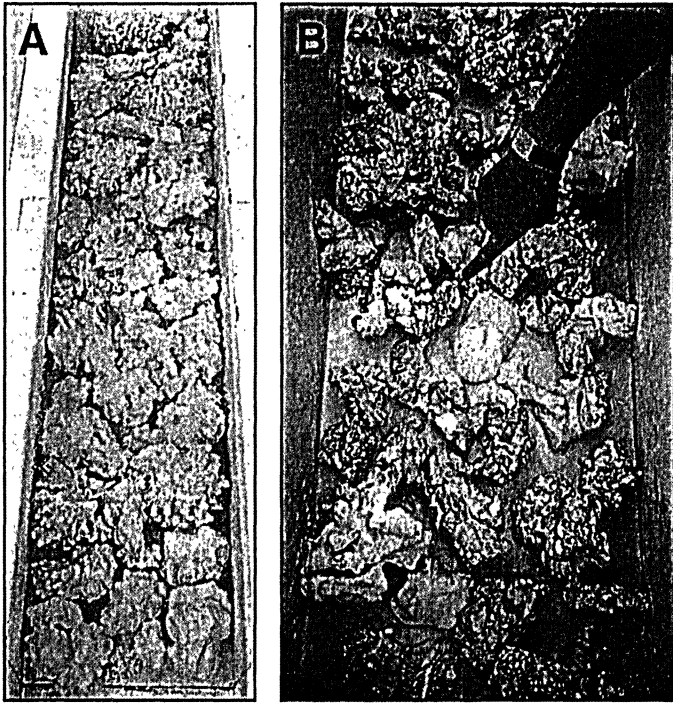


Fig. 5. Gypsum-coated coral skeletons at the beginning of an experiment (A) and well after the experiment has finished (B). Note the relatively fast dissolution of gypsum at the tips of the coral.

surface (No. 60 sandpaper). Grooves of  $\sim 1$ -mm depth and width were scraped into the otherwise smooth coral-rough surface. The  $St_m$  of the roughened gypsum corals were not different from the smooth gypsum corals. This confirms that small-scale roughness in turbulent flows does not change  $c_f$ ,  $k_s$ ,  $Re_k$ , or  $St_m$ , as predicted by engineering literature (Kays

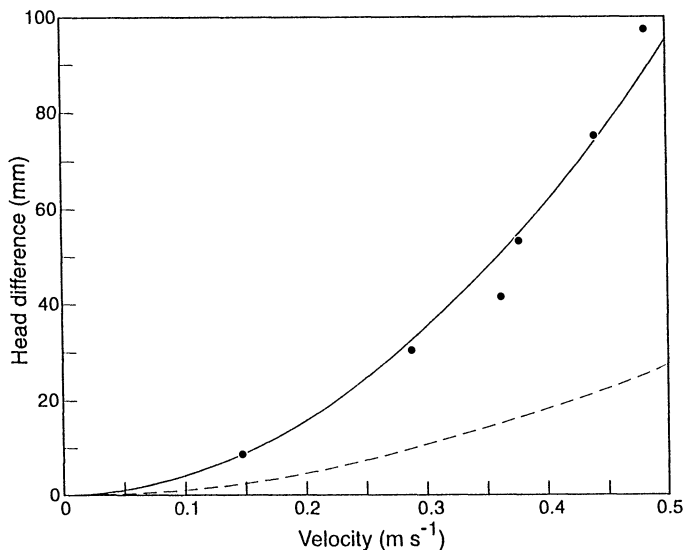


Fig. 6. Head difference vs. velocity for 9 m of gypsum corals A No. 1. Solid points (●) are measured and the solid line is the predicted head, using  $k_s = 0.27$  m in Eq. 20. The dashed line is the predicted head using a measured roughness ( $k' = 8.22$  cm) in Eq. 20.

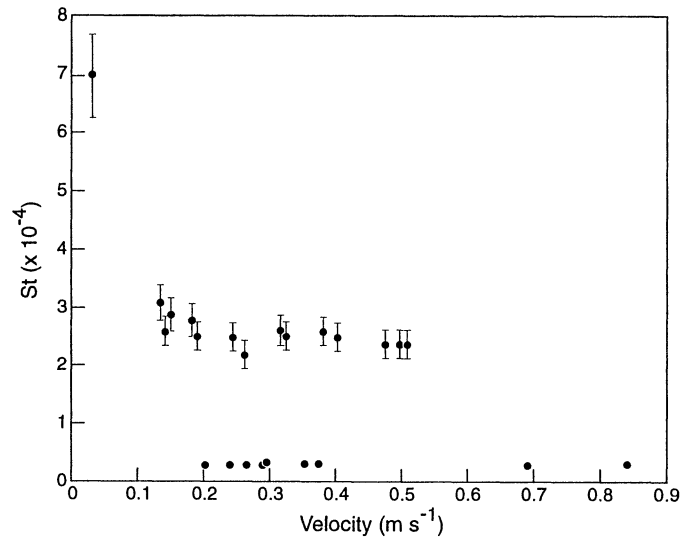


Fig. 7. Stanton number vs. water velocity for dissolution of flat, smooth gypsum surfaces and gypsum-coated coral skeletons (group A). Errors ( $\pm 10\%$  of  $St_m$ ) are based on the variation in measured bulk velocity ( $\pm 5\%$ ) and height of the water ( $\pm 5\%$ ). Errors for smooth surfaces are within the symbols.

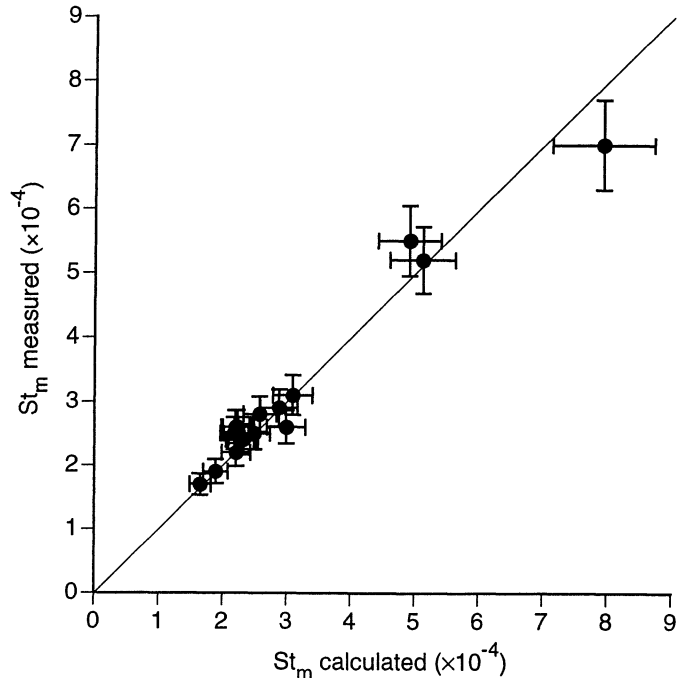


Fig. 8.  $St_m$  measured for gypsum corals A (Table 1) vs.  $St_m$  calculated from measured friction and roughness and using a correlation of heat transfer from sand-roughened pipes (Eq. 25). Each measured  $St_m$  ( $\pm 10\%$ ; vertical error bars) is within the error of  $St_m$  predicted from Eq. 25 ( $\pm 10\%$ ; horizontal error bars).  $St_m$  measured is positively correlated to  $St_m$  predicted ( $P < 0.01$ ). A line of slope 1.0 is shown.

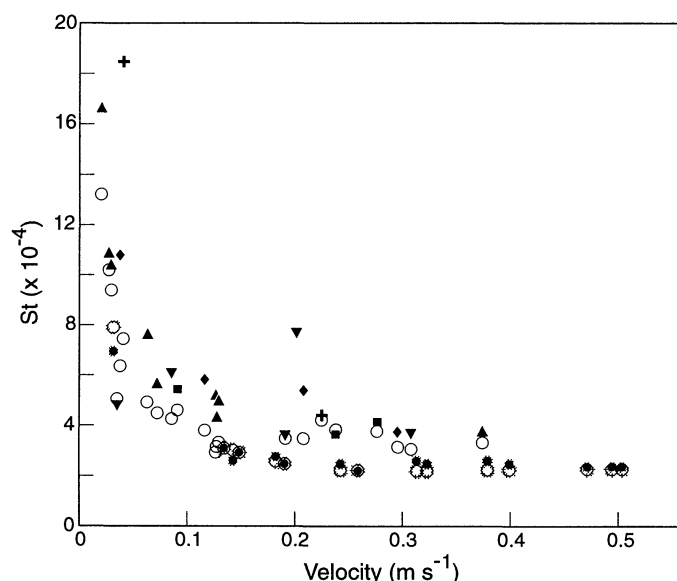


Fig. 9. A comparison of mass transfer on coral-rough surfaces. Solid symbols are measured values; open circles are predicted values using Eq. 25 and 26 and the effective sand-grain roughness,  $k_s$ , calculated from solving Eq. 20. Data for different reef communities from Thomas and Atkinson (1997) are shown as follows: *Porites compressa* (+), *Pocillopora damicornis* (◆), high-relief rubble (■), and low-relief rubble (▼); and data from Larned and Atkinson (1997) for *Dictyosphaeria cavernosa* (▲). Gypsum corals A (●) are highlighted by shading.

and Crawford 1993). However, these comments do not address local variability in transport on rough surfaces; coral branches projected into the flow dissolved gypsum faster than the coral bases close to the bottom of the flume (i.e. see Fig. 5B).

Ammonia uptake for two coral communities, two algal rubble communities (Thomas and Atkinson 1997), and an assemblage of green macroalgae (*Dictyosphaeria cavernosa*; Larned and Atkinson 1997) can be predicted assuming  $C_w = 0$  and using Eq. 9, 23, 25, and 26 (Fig. 9). Thomas and Atkinson (1997) reasoned that the ability for the above equations to predict ammonia uptake indicated that uptake was probably mass-transfer limited. They recognized, however, that  $St_m$  could be higher than predicted values if  $C_w > 0$ . This condition would indicate that the uptake potential of the living coral community was indeed much greater than that of rough engineering surfaces, and Eq. 25 could not be used.

Ammonia  $St_m$  for the above communities are a factor of two higher than  $St_m$  calcium for gypsum dissolution. (Fig. 9). This factor of two is explained by the faster diffusion of ammonia relative to calcium and hence a different  $Sc$  (Eq. 9). Even though  $St_m$  for gypsum dissolution and ammonia uptake are of different magnitudes, they both fit Eq. 25 and are therefore mass-transfer limited.

Thomas and Atkinson (1997) underestimate  $St_m$  at low velocities, which could be attributed to their use of  $k'$  instead of  $k_s$  in Eq. 23.  $St_m$  of gypsum corals A exp. No. 7 coral was overpredicted by 10% and gypsum corals B exp. Nos. 3 and 4 were underpredicted by 17%. We simply need more

low-velocity data to determine the validity of Eq. 25 at low velocities. At this time, however, both ammonia uptake and gypsum dissolution have high  $St_m$  at low velocities, consistent with a purely physical mechanism for mass exchange.

The experiments reported in Fig. 9 were conducted on a variety of different coral assemblages. To demonstrate further that gypsum dissolution and ammonia uptake are mass-transfer limited, ammonia uptake on a living assemblage of reef benthos was measured, then the organisms were dipped in plaster, replaced in the flume, and calcium release measured. The experimental assemblage was comprised of three coral species (*P. compressa*, *M. capitata*, and *Pocillopora meandrina*) and rubble covered with filamentous algae.  $c_f$  was measured at two velocities (0.24 and 0.30  $m s^{-1}$ ). Ammonia uptake was determined by injecting a spike of ammonia (200 ml spike of 26 mM N as  $(NH_4)_2SO_4$ ) into the recirculated seawater and measuring changing concentration of ammonia from 8 to 10 water samples collected over 8 h (for further methods, see Thomas and Atkinson 1997). A control measurement, without the coral community, was conducted to account for ammonia uptake by suspended particles and the sides of the flume. Three gypsum-dissolution experiments at two velocities (0.24, 0.30, and 0.30  $m s^{-1}$ ) were conducted using the techniques described in the methods.

The  $c_f$  for the coral surface during the ammonia-uptake experiment was similar to that during the gypsum dissolution (0.041, 0.042, and 0.040 at velocities of 0.24, 0.30, and 0.30  $m s^{-1}$  vs. 0.050 and 0.043 at 0.26 and 0.35  $m s^{-1}$ , respectively). This indicates no active biological processes that significantly alter  $c_f$ . The  $St_m$  for ammonia uptake (corrected by the control) was  $35 \pm 4 \times 10^{-5}$ , and  $St_m$  for gypsum dissolution was  $18 \pm 1 \times 10^{-5}$ , very close to a factor of two different than would be predicted by Eq. 10 to account for the difference in diffusivities.

Results of this paper corroborate Atkinson and Bilger's (1992) assertion that uptake of nutrients to coral communities is mass-transfer limited. Areas of high water velocity, such as the fore reef, would therefore have the highest potential for the exchange of metabolites. Future work to measure the field values of  $Re$ ,  $c_f$ ,  $h$ ,  $k_s$ , and an analysis of the effects of wave surge should allow prediction of  $St_m$  on the varying physical environments of reefs. At low water velocities there is little risk of damage to coral branches from form drag, so friction from branching ( $c_f$ ) can be high, maximizing  $St_m$ . Thus at low velocities— $[(St_m/c_f)_{rough} \ll (St_m/c_f)_{smooth}]$ —it would be advantageous to have a highly rough form. However, at high water velocities— $[(St_m/c_f)_{rough} \approx (St_m/c_f)_{smooth}]$ —there is no advantage to being rough.

In conclusion, the results of these gypsum dissolution experiments confirm the hypothesis that nutrient uptake to coral reef communities is mass-transfer limited and can be estimated using a heat-transfer correlation to roughened surfaces. Gypsum dissolution from appropriately shaped surfaces can be used as a direct measure of mass transfer, hence estimates of  $St_m$ . The uptake-rate constant,  $St_m U_b$ , can be used to estimate uptake or release rates of metabolites and should vary with different physical environments of reef communities. The friction coefficient of the reef,  $c_f$ , seems to be the most important parameter in determining  $St_m$ .



Clearly, metabolism of coral reefs, and possibly other benthic communities, is a function of the interplay between water motion and biological form.

### References

- ATKINSON, M. J., AND R. W. BILGER. 1992. Effects of water velocity on phosphate uptake in coral reef-flat communities. *Limnol. Oceanogr.* **37**: 273–279.
- , E. KOTLER, AND P. NEWTON. 1994. Effects of water velocity on respiration, calcification and ammonium uptake of a *Porites compressa* community. *Pac. Sci.* **48**: 296–303.
- BANZ, I., AND R. G. LUTHY. 1985. Calcium sulfate solubility in organic-laden wastewater. *J. Environ. Eng.* **111**: 317–335.
- BARTON, A. F. M., AND N. M. WILDE. 1971. Dissolution rates of polycrystalline samples of gypsum and orthorhombic forms of calcium sulphate by a rotating disc method. *Faraday Soc. Trans.* **67**: 3590–3597.
- BILGER, R. W., AND M. J. ATKINSON. 1992. Anomalous mass transfer of phosphate on coral reef flats. *Limnol. Oceanogr.* **37**: 261–272.
- , AND ———. 1995. Effects of nutrient loading on mass transfer rates to a coral-reef community. *Limnol. Oceanogr.* **40**: 279–289.
- CHOW, V. T. 1959. *Open-channel hydraulics*. McGraw-Hill. 680 p.
- DAWSON, D. A., AND D. TRASS. 1972. Mass transfer at rough surfaces. *Int. J. Heat Mass Transfer* **15**: 1317–1336.
- DIPPREY, D. F., AND D. H. SABERSKY. 1963. Heat and momentum transfer in smooth and rough tubes at various Prandtl numbers. *Int. J. Heat Mass Transfer* **6**: 329–353.
- GRASSHOFF, K., M. EHRHARDT, AND K. KREMLING. 1983. *Methods of seawater analysis*, 2nd ed. Verlag Chemie.
- HAALAND, S. E. 1983. Simple and explicit formulas for the friction factor in turbulent pipe flow. *J. Fluid Eng.* **105**: 89–90.
- HARDIE, L. A. 1967. The gypsum-anhydrite equilibrium at one atmosphere pressure. *Am. Min.* **52**: 171–200.
- JOHN, J. E. A., AND W. L. HABERMAN. 1988. *An introduction to fluid dynamics*, 3rd ed. Prentice Hall.
- JOKIEL, P. L., AND J. I. MORRISSEY. 1993. Water motion on coral reefs: Evaluation of the “clod card” technique. *Mar. Ecol. Prog. Ser.* **93**: 175–181.
- KAYS, M. W., AND M. E. CRAWFORD. 1993. *Convective heat and mass transfer*, 3rd ed. McGraw-Hill.
- LARNED, S., AND M. J. ATKINSON. 1997. Effect of water velocity on  $\text{NH}_4$  and  $\text{PO}_4$  uptake and nutrient-limited growth in the macroalga *Dictyosphaeria cavernosa*. *Mar. Ecol. Prog. Ser.* **157**: 295–302.
- LI, Y., AND S. GREGORY. 1974. Diffusion of ions in sea water and deep-sea sediments. *Geochim. Cosmochim. Acta* **38**: 703–714.
- SCHLICHTING, H. 1979. *Boundary layer theory*, 7th ed. McGraw-Hill.
- SHAW, D. A., AND T. J. HANRATTY. 1977. Turbulent mass transfer rates to a wave for large Schmidt numbers. *AIChE J.* **23**: 28–37.
- STEWART, W. E. 1987. Forced convection: Asymptotic forms for laminar and turbulent transfer rates. *AIChE J.* **23**: 28–37.
- THOMAS, F. I. M., AND M. J. ATKINSON. 1997. Ammonia uptake of coral reefs: Effects of surface roughness and water velocity on mass-transfer. *Limnol. Oceanogr.* **42**: 81–88.
- THOMPSON, T. L., AND E. P. GLENN. 1994. Plaster standards to measure water motion. *Limnol. Oceanogr.* **39**: 1768–1779.

Received: 22 July 1996

Accepted: 7 May 1997